

Extension of MC²-3 for Generation of Multigroup Cross Sections in Thermal Energy Range

B. K. Jeon^a, W. S. Yang^a, Y. S. Jung^{a,b} and C. H. Lee^b

^a Purdue University, 400 Central Drive, West Lafayette, IN, 47907, yang494@purdue.edu

^b Argonne National Laboratory, 9700 South Cass Avenue, Lemont, IL, 60439

Abstract - This paper presents the new computational capability of MC²-3 for generation of multigroup cross section in thermal energy range. The multi-group cross section generation code MC²-3 for fast reactor applications has recently been extended to generate the cross sections for the entire energy range of interest in fission reactors. Thermal scattering matrices and interaction cross section libraries for the energy range from 10⁻⁵ eV to 5.0 eV were prepared with the NJOY code in a 1700 group structure. The slowing-down and transport calculation capabilities of MC²-3 were extended to 10⁻⁵ eV in compliance with the new thermal group cross section libraries. Numerical tests were for LWR fuel pin and assembly problems. The 3478-group neutron spectra obtained with MC²-3 agreed well with MCNP6 results. The eigenvalue error was less 160 pcm and the pin power error was less than 1.2% compared to MCNP6 results. These results indicate that the modified MC²-3 can generate accurate cross sections for thermal reactor applications.

I. INTRODUCTION

Under the U.S. DOE's Nuclear Energy Advanced Modeling and Simulation (NEAMS) program, an advanced multi-group cross section generation code MC²-3 was developed for fast reactor applications [1]. The MC²-3 code generates composition-dependent multigroup cross sections by solving the neutron transport equation for a homogeneous medium or a slab or cylindrical unit cell problem in a ultrafine (~2,000) or hyperfine (~400,000) group level with detailed modeling of resolved resonances, unresolved resonances, and anisotropic scatterings. In addition, in order to take into account the local heterogeneity effects more accurately, a two-dimensional method of characteristic (MOC) transport solver has recently been incorporated into MC²-3 at Purdue University [2]. MC²-3 has been validated against various fast critical experiments [3] and widely used for multigroup cross section generation for fast reactor designs and analyses.

Motivated by the analysis needs for recent fast reactor designs including local moderated zones or fast and thermal coupled reactors [4, 5], the MC²-3 code has been extended to generate the multigroup cross sections in the thermal energy range as well as in the fast energy range. This new capability can also be utilized to generate multigroup cross sections for thermal reactor applications with detailed slowing down calculation, in particular for those cases where the current lattice calculation with fine-group cross section libraries is not adequate (e.g., BWR assembly with high-void fraction [6]). For a detailed thermal spectrum calculation, the lower energy boundary has been extended from 0.4 eV to 10⁻⁵ eV. Using the NJOY code [7], 1700-group thermal cross section libraries with upscattering have been generated to cover the energy range from 10⁻⁵ eV to 5.0 eV. The existing transport equation solvers have also been modified to comply with the new thermal libraries with upscattering.

In this paper, we present the new thermal cross section generation capability of MC²-3. The thermal cross section libraries and the modified transport solvers are discussed, and

the verification tests results for the KSNP (Korean Standardized Nuclear Plant) UO₂ fuel pin cell [8], LWR MOX fuel pin cell [9], and VERA [10] benchmark problems are presented.

II. METHODOLOGIES

1. Generation of Thermal Cross Section Libraries

Preliminary thermal cross section libraries of MC²-3 were prepared in a 1700-group structure. The energy range from 0.1 eV to 5.0 eV that includes important thermal resonances was divided into 1625 groups to represent the thermal resonances in this energy range almost pointwise. The energy range from 10⁻⁵ eV to 0.1 eV, where the cross sections vary smoothly, was represented by 75 groups. As a result, the total number of ultrafine groups of MC²-3 becomes 3,483: 1,783 fast groups from 5.0 eV to 14.2 MeV and 1,700 thermal groups from 10⁻⁵ eV to 5.0 eV.

The NJOY code was used to generate the thermal scattering matrices and the interaction cross section libraries at the infinite dilute condition and target temperatures based on the ENDF/B VII.0. Fig. 1 illustrates the computational procedure. The utility code for MC²-3 sub-library, named PMCS [11], prepares the NJOY input files and the input file for another utility code to process the NJOY output files. The thermal scattering matrices and cross section libraries are generated using the RECONR, BROADR, THERMR and GROUPE modules of NJOY. The NJOY output-processing tool converts the output files of NJOY (in the GENDF format) in the formats of the thermal cross section libraries of MC²-3.

Since only the thermal scattering matrices are prepared with the NJOY code, the elastic and inelastic scattering cross sections from fast groups to thermal groups are prepared using the MC²-3 algorithms [1] except for hydrogen. For this, the associated routines of MC²-3 have been modified to comply with the thermal group structure. For hydrogen, the

elastic scattering transfer matrix is analytically obtained as:

$$\sigma_s^l(g \rightarrow g') = \frac{\sigma_{sg}}{(1-\alpha)\Delta u} \int_{u_{g-1}^*}^{u_g^*} du' \int_{u_{g-1}^*}^{u_g^*} du P_l[e^{-(u'-u)/2}] e^{-(u'-u)} \quad (1)$$

where σ_s^l is the l -th moment Legendre expansion coefficient of the scattering transfer matrix from group g to g' , and σ_{sg} is the elastic scattering cross section of group g . u_g^* and u_{g-1}^* are energetically reachable boundaries, Δu is the lethargy width, $\alpha = (A-1)^2 / (A+1)^2$, and A is the atomic mass ratio of hydrogen to neutron.

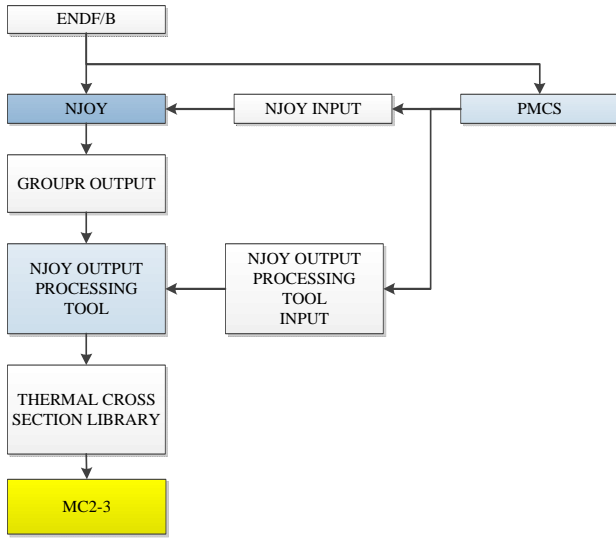


Fig. 1. Procedure to prepare the thermal libraries of MC²-3.

2. Thermal Neutron Transport Calculation in MC²-3

The MC²-3 code solves the consistent P₁ transport equation to determine the fundamental mode spectrum in a homogeneous problem, whereas the Collision Probability Method (CPM) is used to solve one-dimensional (1-D) slab and cylindrical geometry problems. As mentioned in the introduction, a two-dimensional (2-D) MOC solver has been implemented to solve 2-D pin cell and lattice problems. In this MOC solver, anisotropic scattering is modeled up to P₃, whereas the current CPM module of MC²-3 is limited to the isotropic scattering source with optional transport correction.

In order to determine the self-shielded UFG cross sections by taking into account the heterogeneity effect, isotopic escape cross sections are calculated. The Tone's method [12] is employed for 1-D geometries to calculate the isotopic escape cross sections. For 2-D problems, the isotopic escape cross sections are calculated by solving the fixed source transport problem [13]:

$$\Omega \cdot \nabla \psi_{1,r}^g(\mathbf{r}, \Omega) + \Sigma_r^g(\mathbf{r}) \psi_{1,r}^g(\mathbf{r}, \Omega) = \sum_{k \neq r} N_k(\mathbf{r}) \sigma_{t,k}^g(\mathbf{r}) \quad (2)$$

$$\Omega \cdot \nabla \psi_{2,r}^g(\mathbf{r}, \Omega) + \Sigma_r^g(\mathbf{r}) \psi_{2,r}^g(\mathbf{r}, \Omega) = N_r(\mathbf{r}) \quad (3)$$

Using solution of two fixed source problems, the escape cross section for the self-shielded group g cross section of resonant isotope r in a region i can be computed as:

$$\Sigma_{e,r,i}^g = N_{r,i} \frac{\int_{V_i} dV \int_{4\pi} d\Omega \psi_{1,r}^g(\mathbf{r}, \Omega)}{\int_{V_i} dV \int_{4\pi} d\Omega \psi_{2,r}^g(\mathbf{r}, \Omega)} - \sum_{k \neq r} N_k \sigma_{t,k,i}^g \quad (4)$$

For the calculation of thermal spectrum, the 2-D MOC transport solver as well as the homogeneous and 1-D CPM solvers has been extended to comply with the thermal group cross sections and to perform the upscattering iterations in the thermal energy range. The Gauss-Seidel method is used for the upscattering iteration. Fig. 2 shows the overall computational flow of MC²-3 to generate multigroup cross sections.

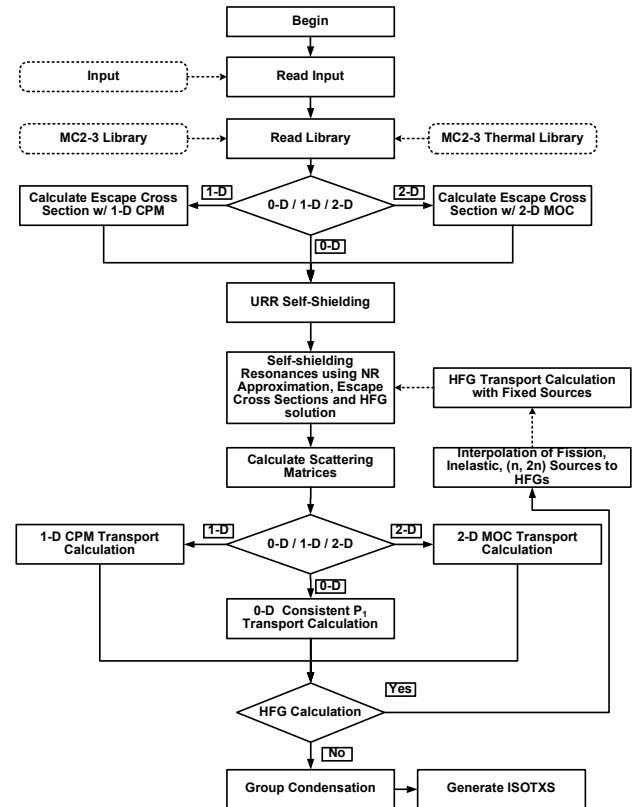


Fig. 2. Overall computational flow of MC²-3

As mentioned above, the spectrum calculation is performed in the ultrafine group (UFG) or hyperfine group (HFG) level. In the UFG calculation, the self-shielded cross sections are determined by the numerical integration of pointwise cross section based on the narrow resonance (NR) approximation as:

$$\bar{\sigma}_{xg}^i = \int_{\Delta u_g} \frac{\sigma_x^i(u)}{\Sigma_i(u)} du / \int_{\Delta u_g} \frac{1}{\Sigma_i(u)} du \quad (5)$$

where Δu_g is the lethargy width of group g , and $\bar{\sigma}_{xg}^i$ is the effective cross section of group g for reaction type x of isotope i .

Since the NR approximation assumes that the resonance width is much smaller than the average energy loss of neutron per scattering, the NR approximation is only valid above a few hundred eV. The errors in the ultrafine group cross sections due to the NR approximation can be eliminated by using the HFG calculation option in the resolved resonance range. In this case, the self-shielded UFG cross sections are recalculated using the HFG flux distribution. Anisotropic elastic scattering sources are directly incorporated in the HFG calculation, but the fission, inelastic scattering and (n,2n) sources are interpolated from the corresponding UFG sources.

III. NUMERICAL RESULTS

1. Fuel Pin Cell Problems

As an initial verification test of the thermal spectrum calculation capability of MC²-3, homogeneous compositions

and 2-D pin cell problems for UO₂ and MOX fuels were solved, and the results were compared with the MCNP6 solutions. Both MC²-3 and MCNP6 calculations were performed using the ENDF/B VII.0 data. The MCNP6 calculations were performed with 10,000 active cycles and 10,000 histories per cycle.

Table I compares the k-infinity values determined with MC²-3 and MCNP6 for the homogenized compositions of UO₂ and MOX pin cell problems. Here, MC²-3 w/ HFG indicates the MC²-3 UFG solution with the self-shielded UFG cross sections recalculated with the HFG flux calculation. It can be seen that the MC²-3 results agree well with the MCNP6 solutions and that the HFG calculation improves the accuracy by reducing the errors resulting from the NR approximation. Differences in the UFG (i.e., 3,483 groups) fission cross sections of ²³⁵U and ²⁴⁹Pu from MCNP6 results are shown in Figs. 3 and 4, respectively, and those in the capture cross sections of ²³⁸U and ²⁴⁹Pu are shown in Figs. 5 and 6, respectively. In general, the HFG calculation improves the accuracy of UFG cross sections. In the resolved resonance region, the cross sections obtained with the HFG calculation agree well with the MCNP6 results except for a few energy groups where the errors are up to 5%. However, these discrepancies do not affect the eigenvalue results as shown in Table I.

Table I. Eigenvalues of MC²-3 and MCNP6 for homogenized compositions of UO₂ and MOX fuel pin cell problems.

Case	Fuel/moderator densities (g/cm ³) and temperatures	Code	k-infinity	Δk (pcm)
KSNP UO ₂ fuel pin [8]	10.061/0.660 300K/300K	MCNP6	1.08949 (6)	-
		MC ² -3 w/o HFG	1.09091	142
		MC ² -3 w/ HFG	1.08989	40
LWR MOX fuel pin [9]	10.300/0.660 300K/300K	MCNP6	1.13225 (6)	-
		MC ² -3 w/o HFG	1.13462	237
		MC ² -3 w/ HFG	1.13378	152

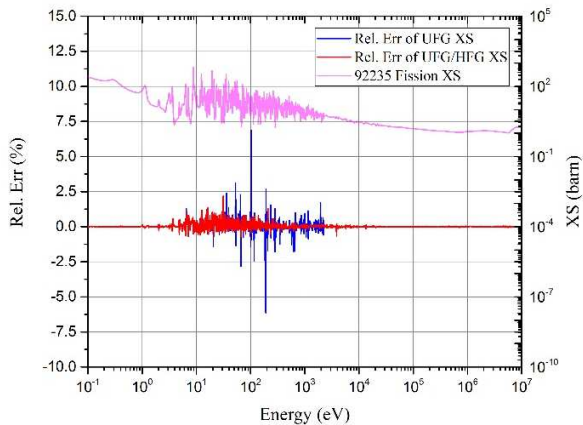


Fig. 3. Comparison of UFG fission cross sections of ²³⁵U between MC²-3 and MCNP6 for LWR MOX fuel pin cell problem.

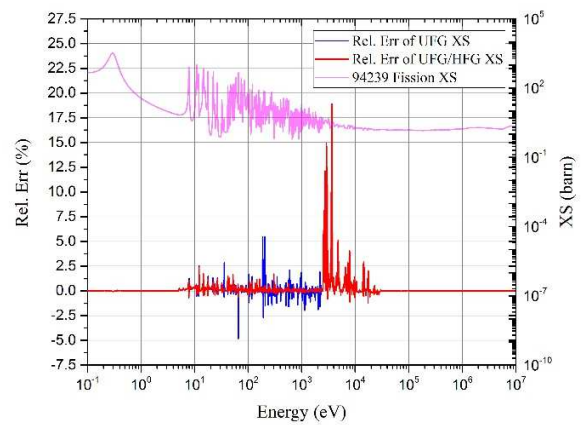


Fig. 4. Comparison of UFG fission cross sections of ²³⁹Pu between MC²-3 and MCNP6 for LWR MOX fuel pin cell problem.

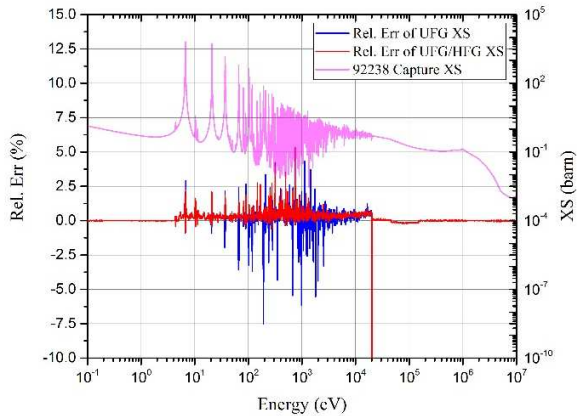


Fig. 5. Comparison of UFG capture cross sections of ^{238}U between MC²-3 and MCNP6 for LWR MOX fuel pin cell problem.

It is also observed that in the unresolved resonance range, MC²-3 yields a smaller absorption cross section and a larger fission cross section for ^{239}Pu than MCNP6. These differences are attributed to different unresolved resonance self-shielding methods of MC²-3 and MCNP6 (i.e., the direct integration method vs. the probability table method). These differences in ^{239}Pu isotope cross sections make the difference in k-infinity between MC²-3 and MCNP6 larger for the MOX problem than the UO₂ problem.

Figs. 7 and 8 compare the UFG neutron spectra obtained with MC²-3 and MCNP6. It can be seen that the spectra obtained from MC²-3 with HFG calculation agree well with the MCNP6 solutions.

Table II presents the k-infinity values calculated with MC²-3 and MCNP6 for two-dimensional UO₂ and MOX fuel pin cell problems. The 2-D MOC calculations of MC²-3 were performed with a ray spacing of 0.025 cm, 32 azimuthal

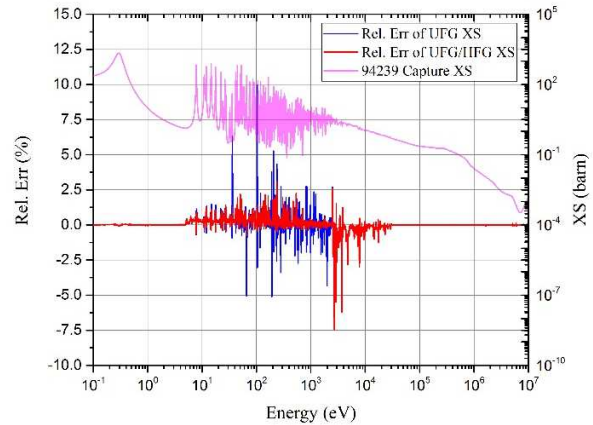


Fig. 6. Comparison of UFG capture cross sections of ^{239}Pu between MC²-3 and MCNP6 for LWR MOX fuel pin cell problem.

angles and 4 polar angles (for $\pi/2$). Anisotropic scattering was modeled up to P₃. It can be seen that the k-infinity values of MC²-3 agree well with the MCNP6 results. The effect of HFG calculation is smaller in each 2-D problem than in the corresponding homogenized problem because of the reduced energy self-shielding effect due to the reduced flux level in the fuel. It is also noted that the MC²-3 results approach the MCNP6 solutions with increasing order of anisotropic scattering. This is consistent with the observation reported in Ref. [14].

Figs. 9 and 10 compare the cell-averaged UFG spectra obtained from MC²-3 calculations (with P₂ scattering order) with MCNP6 results for the 2-D UO₂ and MOX fuel pin cell problems, respectively. It can be seen that the spectra calculated with MC²-3 agree well with the MCNP6 solutions. These results indicate that the transport solver of MC²-3 can provide an accurate solution for 2-D problems.

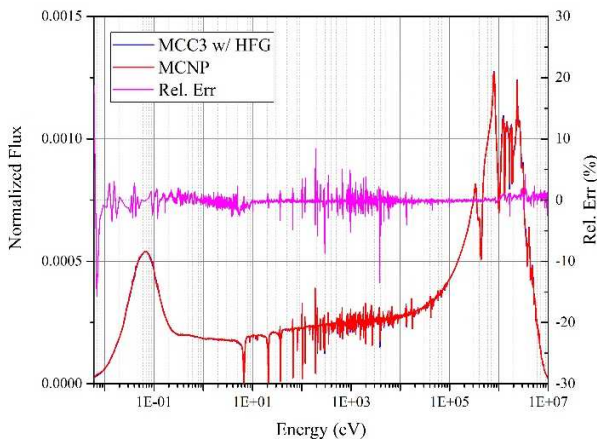


Fig. 7. UFG spectrum of homogenized KSNP UO₂ fuel pin cell problem.

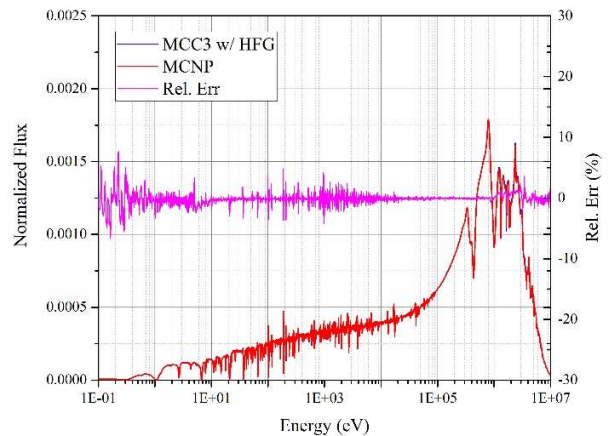


Fig. 8. UFG spectrum of homogenized LWR MOX fuel pin cell problem

Table II. Eigenvalues of MC²-3 and MCNP6 for 2-D UO₂ and MOX fuel pin cell problems.

Case	Fuel/moderator densities (g/cm ³) and temperatures	Code	k-infinity	Δk (pcm)
KSNP UO ₂ fuel pin [8]	10.061/0.660 300K/300K	MCNP6	1.16679 (5)	
		MC ² -3 (P ₁) w/o HFG	1.16576	-103
		MC ² -3 (P ₁) w/ HFG	1.16580	-99
		MC ² -3 (P ₂) w/o HFG	1.16609	-70
		MC ² -3 (P ₂) w/ HFG	1.16614	-65
		MC ² -3 (P ₃) w/o HFG	1.16609	-70
		MC ² -3 (P ₃) w/ HFG	1.16614	-65
LWR MOX fuel pin [9]	10.300/0.660 300K/300K	MCNP6	1.22609 (6)	
		MC ² -3 (P ₁) w/o HFG	1.22390	-220
		MC ² -3 (P ₁) w/ HFG	1.22408	-201
		MC ² -3 (P ₂) w/o HFG	1.22569	-40
		MC ² -3 (P ₂) w/ HFG	1.22586	-23
		MC ² -3 (P ₃) w/o HFG	1.22569	-40
		MC ² -3 (P ₃) w/ HFG	1.22586	-23

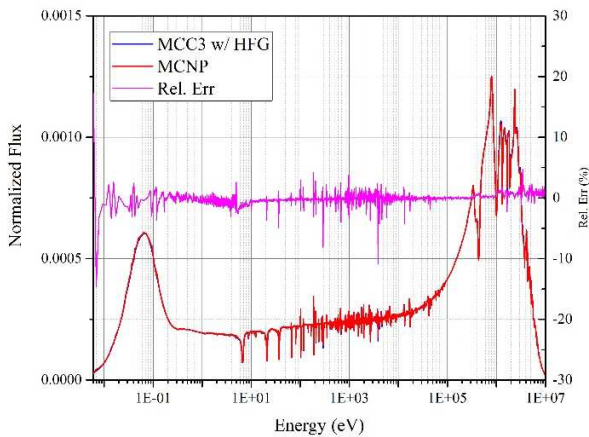


Fig. 9. Cell-averaged UFG spectrum of KSNP UO₂ fuel pin cell problem.

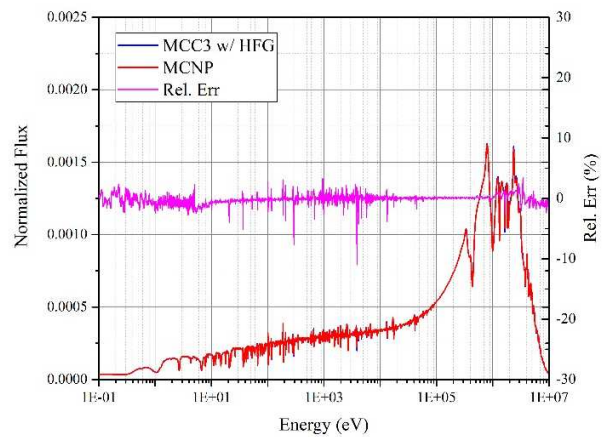


Fig. 10. Cell-averaged UFG spectrum of LWR MOX fuel pin cell problem.

2. VERA Benchmark Problem

The modified MC²-3 was also tested for the VERA PWR fuel lattice problems, which are characterized by 17 x 17 fuel assemblies including several guide tube. The layout of these lattice problems is provided in Fig. 11, and detailed specifications can be found in Ref. [9]. The 2-D MOC calculations of MC²-3 were performed with a ray spacing of 0.05 cm, 32 azimuthal angles and 4 polar angles (for $\pi/2$). In order to perform the slowing down calculations for assemblies, the UFG cross section sets including the scattering matrices need to be stored during the computation, which poses a huge memory requirement. In this work, the region-dependencies of UFG cross sections for fuel pins were approximately considered by grouping them into two sets: the fuel rods adjacent to the guide tube and the remaining ones. For the annular regions of fuel pin that have the same radial location and the cross section group, a single set of escape cross sections were obtained by averaging their variations. To

tackle the memory issue in the lattice calculation, the effective assembly calculation scheme using an intermediate group structure is currently being investigated.

Since the UFG cross section errors induced from the NR approximation are small for UO₂ fuel, the HFG calculations were not invoked for the VERA benchmark problems. P₂ anisotropic scattering was used based on the pin cell results shown in Table II, indicating that P₂ anisotropic scattering is sufficient for typical LWR fuel pin cells. The MCNP6 calculations were performed with 10,000 active cycles and 100,000 histories per cycle to have a relative error of pin power less than 0.04%.

Table III presents the k-infinity values of MC²-3 and MCNP6 for the 2-D pin cell and lattice problems in hot zero power (HWP) condition at the beginning of cycle (BOC) of the VERA benchmark problems. The maximum difference in k-infinity between MCNP6 and MC²-3 results is -124 pcm for pin cell problems (P1D), and -143 pcm for assembly lattice problems (P2D). These results indicate that the MC²-3

code well reproduces the reference k-infinity results of MCNP6 for various lattice problems.

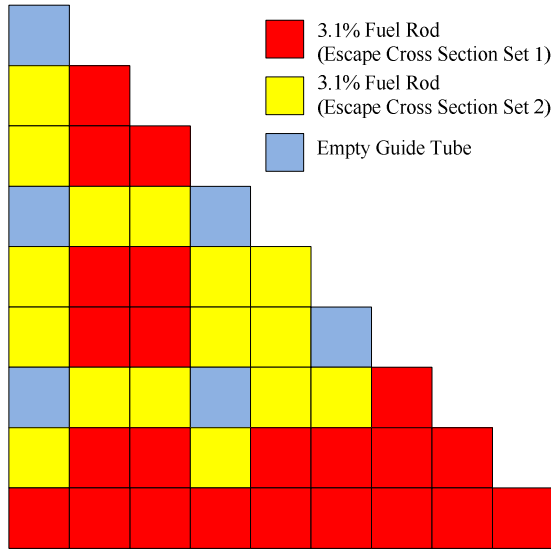


Fig. 11. Lattice layout for VERA benchmark problems (octant symmetry)

Table III. Eigenvalues of MC²-3 and MCNP6 for 2-D pin cell (P1A through P1D) and lattice (P2A through P2D) problems in HZP condition at BOC of VERA benchmarks.

Case	Fuel/moderator densities (g/cm ³) and temperatures	Code	k-infinity	Δk (pcm)
P1A	10.257/0.743 565K/565K	MCNP6	1.18654 (2)	-
		MC ² -3 (P ₂)	1.18667	13
P1B	10.257/0.661 600K/600K	MCNP6	1.18182 (2)	-
		MC ² -3 (P ₂)	1.18180	-1
P1C	10.257/0.661 900K/600K	MCNP6	1.17161 (2)	-
		MC ² -3 (P ₂)	1.17078	-83
P1D	10.257/0.661 1200K/600K	MCNP6	1.16310 (2)	-
		MC ² -3 (P ₂)	1.16186	-124
P2A	10.257/0.743 565K/565K	MCNP6	1.18193 (2)	-
		MC ² -3 (P ₂)	1.18105	-88
P2B	10.257/0.661 600K/600K	MCNP6	1.18284 (2)	-
		MC ² -3 (P ₂)	1.18213	-71
P2C	10.257/0.661 900K/600K	MCNP6	1.17350 (2)	-
		MC ² -3 (P ₂)	1.17246	-104
P2D	10.257/0.661 1200K/600K	MCNP6	1.16568 (2)	-
		MC ² -3 (P ₂)	1.16425	-143

Comparisons of pin-by-pin fission power distribution between MCNP6 and MC²-3 are shown in Fig. 12 through 15. It can be seen that MC²-3 power distributions agree well with the MCNP6 solutions. The maximum and RMS errors of pin-by-pin fission power for P2A through P2D fuel assemblies are 1.137% and 0.485%, respectively. The relatively large errors are observed in the vicinity of guide tubes where the

escape cross sections deviate substantially from the average value. The accuracy of pin-power can be further improved by employing more detailed escape cross sections for each pin.

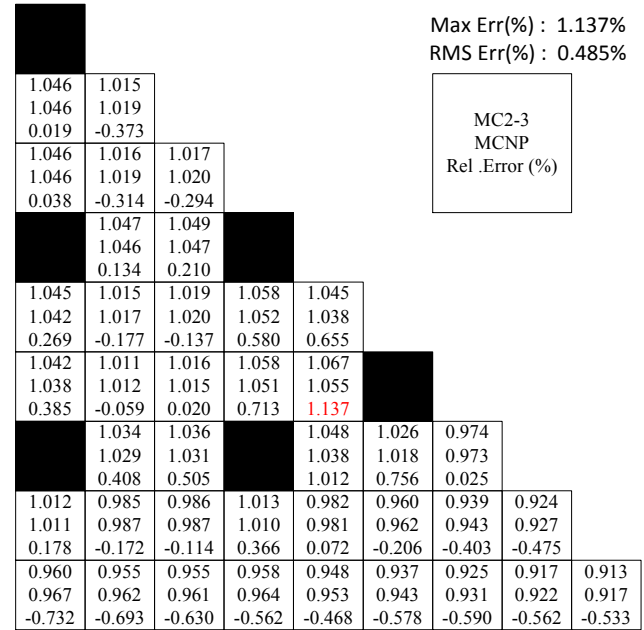


Fig. 12. Comparison of pin-by-pin fission power distribution between MC²-3 and MCNP6 for P2A lattice problem. (Octant symmetry)

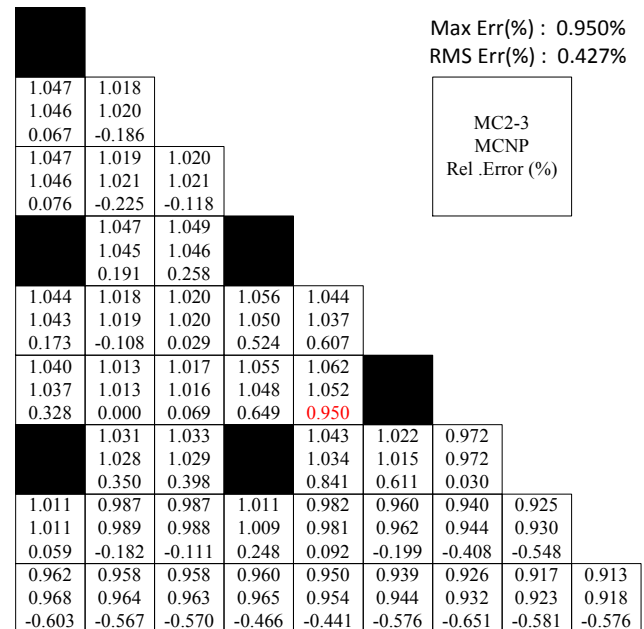


Fig. 13. Comparison of pin-by-pin fission power distribution between MC²-3 and MCNP6 for P2B lattice problem. (Octant symmetry)

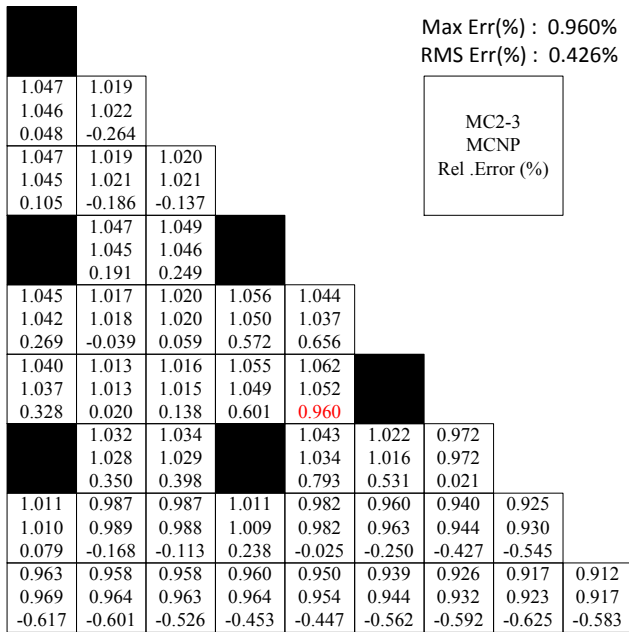


Fig. 14. Comparison of pin-by-pin fission power distribution between MC²-3 and MCNP6 for P2C lattice problem. (Octant symmetry)

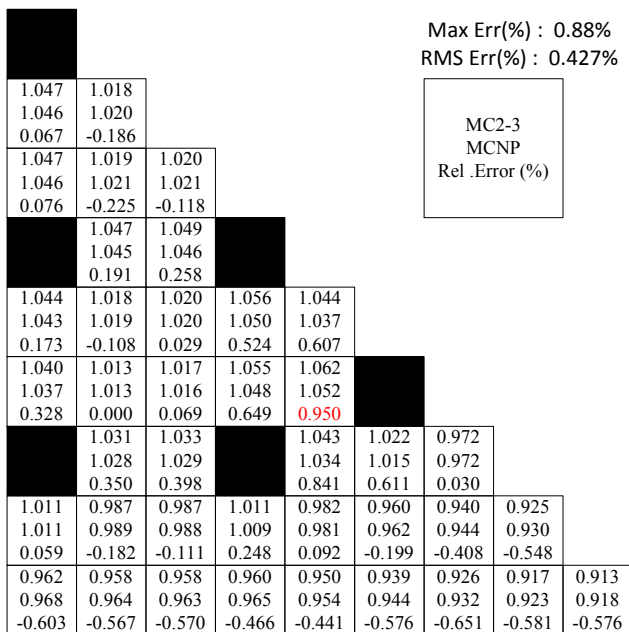


Fig. 15. Comparison of pin-by-pin fission power distribution between MC²-3 and MCNP6 for P2D lattice problem. (Octant symmetry)

IV. CONCLUSIONS

Motivated by the analysis needs for recent fast reactor designs including local moderated zones or fast and thermal coupled reactors [4,5], the MC²-3 code has been extended to generate the multigroup cross sections in the thermal energy range as well as in the fast energy range. Thermal cross section libraries for the energy range from 10⁻⁵ eV to 5.0 eV have been prepared in a 1700-group structure by representing the thermal resonances almost pointwise. The transport solvers of MC²-3 have also been modified to comply with the thermal group cross sections and to perform the upscattering iterations in the thermal energy range.

The thermal spectrum calculation capability of MC²-3 has been tested using the VERA fuel pin and lattice benchmark problems [10] as well as simple UO₂ and MOX fuel pin problems [8,9]. It was observed that the eigenvalues and flux distributions of MC²-3 generally agree well with the corresponding MCNP6 Monte Carlo solutions. For homogeneous problems, the HFG solution is generally required to reduce the error in self-shielded UFG cross sections caused by the NR approximation. However, this error is naturally reduced in 2-D problems with the aid of spatial self-shielding effect in the fuel region. It was also observed that P₂ anisotropic scattering calculation improves the accuracy significantly compared to the P₁ calculation. Thus, the power distributions obtained by MC²-3 are in a good agreement with the MCNP6 results. These results suggest that the new thermal spectrum calculation capability is working properly and the 1700-group thermal cross section libraries are adequate. In the future, work will be focused on reducing the computational time and memory requirements for 2-D transport calculations since the current 2-D MOC assembly calculation in 3,483 energy groups is very costly in time and memory.

ACKNOWLEDGMENTS

This work was supported by the U.S. Department of Energy under Contract number DE-AC02-06CH11357.

REFERENCES

1. C. H. LEE and W. S. YANG, "MC²-3: Multigroup Cross Section Generation Code for Fast Reactor Analysis," Argonne National Laboratory, ANL/NE-11-41 (2011).
2. Y. S. JUNG and W. S. YANG, "A Consistent CMFD Formulation for Acceleration of Neutron Transport Calculations Based on Finite Element Method," *Nucl. Sci. Eng.*, **185**, 307 (2017).
3. C. H. LEE and W. S. YANG, "Verification and Validation of Multigroup Cross Section Generation Code MC²-3 for Fast Reactor System," *Trans. Am. Nucl. Soc.*, **106**, 711 (2012).

4. C. GRANDY et al., "FASTER Test Reactor Preconceptual Design Report," Argonne National Laboratory, ANL/ART-40, (2016).
5. G. YOUINOU et al., "VCTR: A Versatile Coupled Test Reactor Concept," Idaho National Laboratory, INL/EXT-16-38852 (2016).
6. K. S. KIM, "Issues on BWR with high void fraction," Private communication, Oak Ridge National Laboratory (2016).
7. R. E. MACFARLANE and A. C. KAHLER, "Methods for Processing ENDF/B-VII with NJOY," *Nuclear Data Sheet*, **111**, 2739 (2010).
8. H. J. SHIM et al, "Evaluation of CASMO-3 and HELIOS for Fuel Assembly Analysis from Monte Carlo Code," Korea Atomic Energy Research Institute, KAERI/TR-3417/2007, (2007).
9. A. YAMAMOTO et al, "Benchmark Problem Suite for Reactor Physics Study of LWR Next Generation Fuels", *J. Nucl. Sci. Technol.*, **39**, No.8, 900 (2002).
10. A. T. GODFREY, "VERA Core Physics Benchmark Progression Problem Specifications, Revision 4", CASL, CASL-U2012-0131-004, August 31 (2014).
11. B. K. JEON, W. S. YANG and C. H. LEE, "Improved Gamma Yield and Interaction Cross-Section Libraries of MC²-3," *Trans. Am. Nucl. Soc.* **115**, 1299-1302 (2016).
12. T. TONE, "A Numerical Study of Heterogeneity Effects in Fast Reactor Critical Assemblies," *J. Nucl. Sci. Technol.*, **12**, 467 (1975).
13. C. H. LEE and W. S. YANG, "An improved Resonance Self-Shielding Method for Heterogeneous Fast Reactor Assembly and Core Calculations," *In Proc. M&C 2013*, Sun Valley, ID, USA, May 5-9, 2013, on CD-ROM (2013).
14. A. YAMAMOTO et al, "Simplified Treatments of Anisotropic Scattering in LWR Core Calculations", *J. Nucl. Sci. Technol.*, **45**, No.3, 217 (2008).